Turkish J. Eng. Env. Sci.
29 (2005) , 113 – 128.

On the Application of von Mises' Yield Criterion to a Class of Plane Strain Thermal Stress Problems

Ahmet N. ERASLAN
Middle East Technical University, Department of Engineering Sciences
Ankara-TURKEY
e-mail: aeraslan@metu.edu.tr
Hakan ARGESO
Başkent University, Department of Mechanical Engineering
Ankara-TURKEY

Received 10.11.2004

Abstract

A computational model is developed to estimate thermal stresses in nonlinearly hardening elastic-plastic axisymmetric systems in cylindrical polar coordinates. The model is based on von Mises' yield criterion, total deformation theory and Swift's hardening law. Various numerical examples including plane strain and generalized plane strain problems in cylinders and tubes are handled. Comparisons are made with existing analytical solutions employing Tresca's yield criterion for elastic-ideally plastic and elastic-linearly hardening systems. Parametric analyses are carried out to investigate the effect of important model parameters on the stresses and deformations.

Key words: Thermoelastoplasticity, Nonlinear strain hardening, von Mises' criterion, Residual stresses.

Introduction

Analysis of thermally induced deformations of rods, tubes, disks, spherical shells and other structures is of great importance in engineering design and operation (Boley and Weiner, 1960; Timoshenko and Goodier, 1970; Uğural and Fenster, 1995). Since in general, to better utilize the material, plastic deformation may be admitted to some extent, recent studies have focused on elastic-plastic treatment of thermal behavior. A special case, in which thermal deformations are caused by a prescribed symmetrical temperature distribution or internal energy generation in systems that can be treated under plane-strain presupposition, has been the topic of numerous investigations. The elastic-plastic deformation occurring in a perfectly plastic cylinder having fixed ends subjected to a uniform temperature inside its cylindrical core was studied by Orcan and Gamer (1991). Later, Gülgeç and Orcan (1999) extended the analysis presented in Orcan and Gamer (1991) to include linear strain hardening. In a closely related work, Orcan (1994a) obtained the solution of an elastic-ideally plastic cylindrical rod with uniform internal energy generation. All stages of the elastic-plastic deformation of a uniform heat generating tube with free ends were studied analytically by Orcan and Gülgeç (2001), assuming perfectly plastic material behavior. Recent investigations include the numerical solution of thermal stresses in elastic perfectly plastic tubes considering temperature dependent physical properties by Orcan and Eraslan (2001), an analytical solution of 2-layer tubes for linear hardening by Eraslan *et al.* (2003) and for nonlinear hardening by Eraslan (2003) and an analytical solution considering a convective boundary condition for fixed end cylinders by Eraslan and Orcan (2004). In all these theoretical investigations, Tresca's yield criterion and its associated flow rule were used.

The use of Tresca's yield criterion in elastoplastic analysis for nonhardening or linear hardening materials leads to linear differential equations and hence permits the analytical treatment of the problem. However, in the case of thermoplasticity its use needs separate treatment in each region due to different forms of the yield criterion in different parts of the plastic zone. Due to various combinations of elastic and plastic regions, the analysis depends entirely on the temperature distribution and may change completely if a different temperature distribution is imposed. Moreover, in the case when a plastic region expands over a plastically predeformed region the task becomes quite cumbersome. Hence, to develop an algorithm for a unified treatment for design purposes by the use of Tresca's yield criterion would be a formidable task.

In this work, we suggest a simple computational procedure for the unified treatment of a class of plane strain thermal stress problems taking nonlinear strain hardening into account. The model is based on von Mises' yield criterion, the deformation theory of plasticity and a Swift-type hardening law. A shooting method using Newton iterations with numerically generated tangents is developed for the numerical solution of the nonlinear governing differential equation. The major contributions of the present model are the inclusion of (i) von Mises' yield criterion, (ii) nonlinear isotropic hardening, (iii) any prescribed temperature distribution and (iv) an efficient numerical solution procedure. Furthermore, all combinations of solid and hollow cylinders with fixed and free end conditions can be handled. Small and large values of the hardening parameters can be used without any difficulty.

The results of the computations are compared with the existing analytical solutions based on Tresca's criterion to verify the present computational model. These comparisons indicate that there exists fairly good agreement in the predictions of stress and displacement distributions and relatively poor agreement in plastic strain, predictions for structures made of ideally-plastic and linearly hardening materials. It is also observed that the elastic-plastic interface predicted by Tresca's criterion advances further than that of von Mises and hence, lower fully plastic limits are predicted by Tresca's yield criterion.

Model Development

The elastic equation

The following dimensionless and normalized variables are introduced: Radial coordinate: $\overline{r} = r/b$, inner radius: $\overline{a} = a/b$, normal stress: $\overline{\sigma_j} = \sigma_j/\sigma_0$, normal strain: $\overline{\epsilon}_j = \epsilon_j E/\sigma_0$, radial displacement: $\overline{u} = uE/\sigma_0 b$, heat load: $\overline{Q} = QE\alpha b^2/\sigma_0 k$, coefficient of thermal expansion: $\overline{\alpha} = \alpha E/\sigma_0$, hardening parameter: $H = \eta\sigma_0/E$, with b being the outer radius, σ_0 the yield limit of the material, E the modulus of elasticity, Q the constant rate of internal heat generation, k the thermal conductivity, α the coefficient of thermal expansion and η the hardening parameter. The equations given below are written in terms of these variables. For convenience, the overbar will be dropped.

A state of generalized plane strain and small deformations are presumed. The strain displacement relations: $\epsilon_r = u'$, $\epsilon_\theta = u/r$, the equation of equilibrium in the radial direction

$$\sigma_\theta = (r\sigma_r)', \tag{1}$$

the compatibility relation

$$\epsilon_r = (r\epsilon_\theta)', \tag{2}$$

and generalized Hooke's law

$$\epsilon_r = \epsilon_r^p + \sigma_r - \nu\,(\sigma_\theta + \sigma_z) + \alpha\Delta T, \tag{3}$$

$$\epsilon_\theta = \epsilon_\theta^p + \sigma_\theta - \nu\,(\sigma_r + \sigma_z) + \alpha\Delta T, \tag{4}$$

$$\epsilon_z = \epsilon_z^p + \sigma_z - \nu\,(\sigma_r + \sigma_\theta) + \alpha\Delta T, \tag{5}$$

are valid both in elastic (with plastic strain $\epsilon_i^p = 0$) and in plastic regions. In the equations above, ΔT represents the temperature difference between the local and reference temperatures and a prime indicates differentiation with respect to the nondimensional radial coordinate r. For purely elastic deformations $\epsilon_i^p = 0$. Furthermore, in a state of generalized plane strain $\epsilon_z = \epsilon_0 = \mathit{constant}$ and from Eq. (5) the axial stress is determined as

$$\sigma_z = \epsilon_0 + \nu(\sigma_r + \sigma_\theta) - \alpha\Delta T. \tag{6}$$

Introducing the stress function $Y(r)$ in terms of radial stress as $Y(r) = r\sigma_r$, we obtain from the equation of equilibrium (1), $\sigma_\theta = Y'(r)$. Hence, the total strains become

$$\epsilon_r = \frac{1}{r}(1-\nu^2)Y - \nu(1+\nu)Y' - \nu\epsilon_0 + \alpha(1+\nu)\Delta T, \tag{7}$$

$$\epsilon_\theta = -\frac{\nu}{r}(1+\nu)Y + (1-\nu^2)Y' - \nu\epsilon_0 + \alpha(1+\nu)\Delta T. \tag{8}$$

The elastic equation is obtained upon substitution of ϵ_r and ϵ_θ in the compatibility relation (2). The result is

$$r^2\frac{d^2Y}{dr^2} + r\frac{dY}{dr} - Y = -\frac{\alpha}{1-\nu}r^2\frac{dT}{dr}. \tag{9}$$

This is a Cauchy-Euler nonhomogeneous differential equation and its analytical solution will be used to determine elastic limit heat loads later.

The plastic equation

In the plastic region, the axial stress takes the form

$$\sigma_z = \epsilon_0 - \epsilon_z^p + \nu(\sigma_r + \sigma_\theta) - \alpha\Delta T. \tag{10}$$

Eliminating the axial stress from the total strain expressions (3) and (4) and substituting the results in the compatibility relation (2) leads to the governing differential equation for the plastic region.

$$\begin{aligned} r^2\frac{d^2Y}{dr^2} + r\frac{dY}{dr} - Y = -\frac{\alpha}{1-\nu}r^2\frac{dT}{dr} + \\ \frac{r}{1-\nu^2}\left[\epsilon_r^p - \epsilon_\theta^p - r\left(\frac{d\epsilon_\theta^p}{dr} + \nu\frac{d\epsilon_z^p}{dr}\right)\right]. \end{aligned} \tag{11}$$

Note that in the elastic region the plastic strains ϵ_j^p and hence their derivatives $(\epsilon_j^p)'$ vanish and this equation reduces to the elastic equation given by Eq. (9). Therefore, the stress function Y and its first order derivative Y' are continuous at the elastic-plastic interface, and as a result the continuity of the stress components and the displacement at the elastic-plastic border is satisfied. For this reason, Eq. (11) is, in fact, the governing equation to be integrated for the analysis of thermoelastoplastic response as it switches between elastic and plastic equations. Since the plastic strains are not known *a priori*, Eq. (11) is not convenient to handle the plastic region, and an alternate form, containing explicit expressions for the plastic strains will be derived next using the deformation theory of plasticity.

For plane strain, von Mises' yield criterion takes the form

$$\sigma_y = \sqrt{\frac{1}{2}[(\sigma_r - \sigma_\theta)^2 + (\sigma_r - \sigma_z)^2 + (\sigma_\theta - \sigma_z)^2]}. \tag{12}$$

In the absence of plastic predeformation, using total deformation theory and plastic incompressibility one obtains the plastic strains as

$$\epsilon_r^p = \frac{\epsilon_{EQ}}{\sigma_y}\left[\sigma_r - \frac{1}{2}(\sigma_\theta + \sigma_z)\right], \tag{13}$$

$$\epsilon_\theta^p = \frac{\epsilon_{EQ}}{\sigma_y}\left[\sigma_\theta - \frac{1}{2}(\sigma_r + \sigma_z)\right], \tag{14}$$

$$\epsilon_z^p = \frac{\epsilon_{EQ}}{\sigma_y}\left[\sigma_z - \frac{1}{2}(\sigma_r + \sigma_\theta)\right], \tag{15}$$

where ϵ_{EQ} represents the normalized equivalent plastic strain and according to Swift's hardening law it is related to the yield stress σ_y as

$$\sigma_y = (1 + H\epsilon_{EQ})^{1/m}, \tag{16}$$

and the inverse relation is

$$\epsilon_{EQ} = (\sigma_y^m - 1)\frac{1}{H}, \tag{17}$$

where m is a material parameter intended to simulate nonlinear hardening for the values of $m \neq 1$. The total strain components are obtained by superposition of plastic, elastic and thermal contributions. They become

$$\begin{aligned} \epsilon_r = \quad & \frac{(\sigma_y^m - 1)}{H\sigma_y}\left[\sigma_r - \frac{1}{2}(\sigma_\theta + \sigma_z)\right] + \\ & [\sigma_r - \nu(\sigma_\theta + \sigma_z)] + \alpha\Delta T, \end{aligned} \tag{18}$$

$$\begin{aligned} \epsilon_\theta = \quad & \frac{(\sigma_y^m - 1)}{H\sigma_y}\left[\sigma_\theta - \frac{1}{2}(\sigma_r + \sigma_z)\right] + \\ & [\sigma_\theta - \nu(\sigma_r + \sigma_z)] + \alpha\Delta T, \end{aligned} \tag{19}$$

$$\begin{aligned} \epsilon_z = \epsilon_0 = \quad & \frac{(\sigma_y^m - 1)}{H\sigma_y}\left[\sigma_z - \frac{1}{2}(\sigma_r + \sigma_\theta)\right] + \\ & [\sigma_z - \nu(\sigma_r + \sigma_\theta)] + \alpha\Delta T. \end{aligned} \tag{20}$$

Some algebraic manipulations are necessary before the total strains are substituted in the compatibility relation to obtain the governing equation. First, the derivative of the yield stress σ_y is written in the form

$$\frac{d\sigma_y}{dr} = N_1 + N_2\frac{d\sigma_z}{dr} + N_3\frac{d\sigma_\theta}{dr}, \tag{21}$$

where

$$N_1 = \left[\frac{2\sigma_r - \sigma_\theta - \sigma_z}{2\sigma_y}\right]\frac{d\sigma_r}{dr}, \tag{22}$$

$$N_2 = \frac{2\sigma_z - \sigma_r - \sigma_\theta}{2\sigma_y}, \tag{23}$$

$$N_3 = \frac{2\sigma_\theta - \sigma_r - \sigma_z}{2\sigma_y}. \tag{24}$$

Then Eq. (20) is differentiated with respect to the radial coordinate r by making use of Eq. (21) and $\epsilon_0' = 0$ to give

$$\frac{d\sigma_z}{dr} = \frac{1}{N_8}\left[N_1N_4N_5 - 2H\alpha\sigma_y^2\frac{dT}{dr} + N_6\sigma_y\frac{d\sigma_r}{dr} + (N_3N_4N_5 + N_6\sigma_y)\frac{d\sigma_\theta}{dr}\right], \tag{25}$$

in which the following variables have just been defined:

$$N_4 = \sigma_y^m(m-1) + 1, \tag{26}$$

$$N_5 = \sigma_r + \sigma_\theta - 2\sigma_z, \tag{27}$$

$$N_6 = \sigma_y^m + 2H\nu\sigma_y - 1, \tag{28}$$

$$N_7 = \sigma_y^m + H\sigma_y - 1, \tag{29}$$

$$N_8 = 2N_7\sigma_y - N_2N_4N_5. \tag{30}$$

Substituting the total strains from Eqs. (18) and (19) in the compatibility relation (2) and employing the relations (21) and (25) results in

$$-\frac{rN_1N_4N_9}{2H\sigma_y^2} - \frac{rN_1N_4N_5N_{10}}{2HN_8\sigma_y^2} + r\alpha\left[1 + \frac{N_{10}}{N_8}\right]\frac{dT}{dr} + \left[\frac{3 - 2H(1+\nu)\sigma_y - 3\sigma_y^m}{2H\sigma_y}\right]\sigma_r + \left[1 + \nu + \frac{3(\sigma_y^m - 1)}{2H\sigma_y}\right]\sigma_\theta - \left[\frac{rN_6(N_8 + N_{10})}{2HN_8\sigma_y}\right]\frac{d\sigma_r}{dr} - \left[\frac{r[N_3N_4(N_8N_9 + N_5N_{10}) - \sigma_y(2N_7N_8 - N_6N_{10})]}{2HN_8\sigma_y^2}\right] \times\frac{d\sigma_\theta}{dr} = 0, \tag{31}$$

where

$$N_9 = \sigma_r + \sigma_z - 2\sigma_\theta, \tag{32}$$

$$N_{10} = N_2N_4N_9 + N_6\sigma_y. \tag{33}$$

If all stresses are expressed in terms of the stress function using $\sigma_r = Y/r$, $\sigma_\theta = Y'$, then Eq. (31) can be cast into the general form

$$\frac{d^2Y}{dr^2} = F(r, Y, \frac{dY}{dr}). \tag{34}$$

The substitution of the axial stress σ_z on the right hand side of this equation is achieved by the use of either Eq. (6) or Eq. (20) depending on whether the region is elastic or plastic. In the case of using Eq. (20), a nonlinear iteration is carried out. Eq. (34) constitutes a nonlinear 2-point boundary value problem and can be solved numerically, subject to the following boundary conditions:

$$Y(a) = 0 \text{ and } Y(1) = 0 \text{ for } a \geq 0. \tag{35}$$

Note that while this relation holds for both $a = 0$ and $a > 0$, in the case $a = 0$, $\sigma_r(0) = Y'(0)$, whereas for $a > 0$ then $\sigma_r(a) = Y(a)/a$. For accurate integration of Eq. (34), a nonlinear shooting method using Newton iterations with numerically approximated tangents is used. To this end, we define 2 new variables as $\phi_1(r) = Y$ and $\phi_2(r) = dY/dr$ so that one may obtain the system

$$\frac{d\phi_1}{dr} = \phi_2, \tag{36}$$

$$\frac{d\phi_2}{dr} = F(r, \phi_1, \phi_2). \tag{37}$$

Equations (36) and (37) form a system of initial value problems (IVP) and should be solved starting with the initial conditions $\phi_1(a) = Y(a) = 0$ and $\phi_2(a) = dY/dr|_{r=a}$. Since normally the gradient of Y at $r = a$ is not known, a Newton iteration scheme is used to obtain the correct value of this gradient by requiring $\phi_1(1) = Y(1) = 0$. A double precision version of the state-of-the-art ODE solver LSODE by Hindmarsh (1983) is used for the numerical solution of IVP with the stiff option turned on. An outer iteration loop is performed to determine the value of ϵ_0 in the case that a free end condition is considered. At each iteration, the problem is solved 3 times using ϵ_0^k, $\epsilon_0^k + \Delta_\epsilon$ and $\epsilon_0^k - \Delta_\epsilon$ respectively, and corresponding net axial forces $\int \sigma_z \, dA$ are calculated. A better approximation ϵ_0^{k+1} to the constant axial strain is then obtained from

$$\epsilon_0^{k+1} = \epsilon_0^k - \frac{(2\Delta_\epsilon) \int \sigma_z(\epsilon_0^k) \, dA}{\int \sigma_z(\epsilon_0^k + \Delta_\epsilon) \, dA - \int \sigma_z(\epsilon_0^k - \Delta_\epsilon) \, dA}, \tag{38}$$

where Δ_ϵ stands for a small increment of the order of $\epsilon_0^k/100$. Starting with a reasonable initial estimate of ϵ_0^0, this iteration scheme converges to the result with a sufficient accuracy in only a few iterations.

Preliminary Calculations

The general solution of Eq. (9) is

$$Y(r) = \frac{C_1}{r} + C_2 r - \frac{\alpha}{2(1-\nu)} \left[rT - \frac{I_p(r)}{r} \right], \tag{39}$$

in which C_i represents an arbitrary integration constant, a the inner radius, and

$$I_p(r) = \int_a^r T'(\xi)\xi^2 d\xi. \tag{40}$$

Hence, the stresses and radial displacement are determined as

$$\sigma_r = \frac{C_1}{r^2} + C_2 - \frac{\alpha}{2(1-\nu)} \left[T - \frac{I_p(r)}{r^2} \right], \tag{41}$$

$$\sigma_\theta = -\frac{C_1}{r^2} + C_2 - \frac{\alpha}{2(1-\nu)} \left[T + \frac{I_p(r)}{r^2} \right], \tag{42}$$

$$\sigma_z = 2\nu C_2 + \epsilon_0 - \frac{\alpha T}{1-\nu}, \tag{43}$$

$$\begin{aligned} u = \; & (1+\nu) \left\{ -\frac{C_1}{r} + (1-2\nu) r C_2 - \frac{r\nu\epsilon_0}{1+\nu} \right. \\ & \left. + \frac{\alpha}{2(1-\nu)} \left[rT - \frac{I_p(r)}{r} \right] \right\}. \end{aligned} \tag{44}$$

For a generalized plane strain problem, the axial strain ϵ_0 is constant and its value is determined by requiring that the net axial force F_z must vanish, that is

$$F_z = \int \sigma_z \, dA = 2\pi \int_a^1 \sigma_z r dr = 0, \tag{45}$$

which gives

$$\epsilon_0 = -2\nu C_2 + \frac{2\alpha}{(1-a^2)(1-\nu)} \int_a^1 T(r) r dr. \tag{46}$$

The solution is completed by the application of boundary conditions. For a cylinder, the stresses and displacement must be finite at the axis and the surface may be assumed to be free of traction, that is $\sigma_r(1) = 0$. These conditions lead to

$$C_1 = 0 \quad \text{and} \quad C_2 = \frac{\alpha[T(1) - I_p(1)]}{2(1-\nu)}. \tag{47}$$

For a tube of inner radius a, the boundary conditions used are $\sigma_r(a) = \sigma_r(1) = 0$ giving

$$\begin{aligned} C_1 &= \frac{a^2\alpha[T(a) - T(1) + I_p(1)]}{2(1-a^2)(1-\nu)}, \\ C_2 &= -\frac{\alpha[a^2 T(a) - T(1) + I_p(1)]}{2(1-a^2)(1-\nu)}. \end{aligned} \tag{48}$$

On the other hand, the steady temperature distribution in a uniform heat generating cylinder whose surface is kept at constant reference temperature $T_0 = 0$ is given by Orcan (1994a)

$$T(r) = \frac{Q}{4\alpha}(1 - r^2). \tag{49}$$

Using this temperature distribution and considering a cylinder with fixed ends, $\epsilon_0 = 0$, the elastic stresses are determined as

$$\begin{aligned} \sigma_r &= -\frac{Q(1-r^2)}{16(1-\nu)}, \quad \sigma_\theta = -\frac{Q(1-3r^2)}{16(1-\nu)}, \\ \sigma_z &= -\frac{Q(2-\nu-2r^2)}{8(1-\nu)}. \end{aligned} \tag{50}$$

Yielding commences at the axis of the fixed end cylinder as soon as $\sigma_y \geq 1$. Since the stress state at this location satisfies $\sigma_r = \sigma_\theta > \sigma_z$, von Mises' yield criterion (12) at the limit $\sigma_y = 1$ reduces to

$$1 = \sigma_r(0) - \sigma_z(0) = \sigma_\theta(0) - \sigma_z(0). \tag{51}$$

Accordingly, the elastic limit heat load $Q = Q_1$ is obtained as

$$Q_1 = \frac{16(1-\nu)}{3-2\nu}. \tag{52}$$

It is noted that Tresca's yield criterion leads to an identical result (Eraslan and Orcan, 2004).

For a cylinder with free ends, using Eq. (46) the constant axial strain is determined as $\epsilon_0 = Q/8$.

The above expressions given by Eq. (50) for the radial and circumferential stresses are still valid but the axial stress, which depends on ϵ_0, takes the form

$$\sigma_z = -\frac{Q(1-2r^2)}{8(1-\nu)}. \tag{53}$$

In this case, yielding first begins at the surface ($r = 1$) of the cylinder where the stresses satisfy $\sigma_\theta = \sigma_z > \sigma_r = 0$. Von Mises' yield criterion simplifies to

$$1 = \sigma_\theta(1) = \sigma_z(1), \tag{54}$$

which leads to the elastic limit

$$Q_1 = 8(1-\nu), \tag{55}$$

a result identical to the one obtained by Tresca's criterion (Orcan, 1994a). Hence, for cylinders having the temperature distribution prescribed by Eq. (49) and traction free surface, both von Mises' and Tresca's criteria predict identical elastic limits for fixed as well as free end conditions.

On the other hand, the temperature distribution in a uniform heat generating tube with the inner face insulated and the other kept at zero reference temperature is given by Orcan and Gülgeç (2001)

$$T(r) = \frac{Q}{4\alpha}(1 - r^2 + 2a^2 \ln r). \tag{56}$$

This temperature distribution results in the following expressions for stresses in a tube with fixed ends ($\epsilon_0 = 0$):

$$\sigma_r = \frac{Q\left\{4a^4(1-r^2)\ln a + (1-a^2)[(a^2-r^2)(1-r^2) - 4a^2r^2\ln r]\right\}}{16r^2(1-a^2)(1-\nu)}, \tag{57}$$

$$\sigma_\theta = -\frac{Q\left\{4a^4(1+r^2)\ln a + (1-a^2)[a^2 - 3r^4 + r^2(1+5a^2+4a^2\ln r)]\right\}}{16r^2(1-a^2)(1-\nu)}, \tag{58}$$

$$\sigma_z = -\frac{Q\left[4a^4\nu\ln a + (1-a^2)(2 - 2r^2 - \nu + 3a^2\nu + 4a^2\ln r)\right]}{8(1-a^2)(1-\nu)}. \tag{59}$$

Yielding commences at the inner surface ($r = a$) of the tube where $\sigma_r = 0 > \sigma_\theta > \sigma_z$. Substituting the stresses from Eqs. (57)-(59) in

$$1 = \sqrt{\sigma_\theta(a)^2 - \sigma_\theta(a)\sigma_z(a) + \sigma_z(a)^2}, \tag{60}$$

and simplifying, the elastic limit heat load is determined to be

$$Q_1 = 8(1-a^2)(1-\nu)/\sqrt{D}, \tag{61}$$

where

$$\begin{aligned} D = {} & (1-a^2)^2\left\{3 - \nu(3-\nu) - 2a^2[3-\nu(7-3\nu)] + a^4[7-3\nu(5-3\nu)]\right\} \\ & +4a^2(1-a^2)\ln a\left\{3 - \nu + a^4(1-\nu)(5-6\nu) - 2a^2[2-\nu(4-\nu)]\right\} \\ & +16a^4(\ln a)^2[1 - a^2(1-\nu) + a^4(1-\nu)^2]. \end{aligned} \tag{62}$$

Note that, according to Tresca's yield criterion, the yield condition reads $1 = \sigma_r(a) - \sigma_z(a)$, which gives the limit

$$Q_1 = \frac{8(1-a^2)(1-\nu)}{(1-a^2)[2-\nu-a^2(2-3\nu)] + 4\ln a[a^2 - a^4(1-\nu)]}. \tag{63}$$

If the ends of the tube are free, then the axial strain is calculated as

$$\epsilon_0 = \frac{Q}{8}\left[1 - 3a^2 - \frac{4a^4\ln a}{1-a^2}\right]. \tag{64}$$

Then the axial stress component becomes

$$\sigma_z = -\frac{Q\left[4a^4 \ln a + (1-a^2)(1+3a^2-2r^2+4a^2\ln r)\right]}{8(1-a^2)(1-\nu)}. \tag{65}$$

For a tube with free ends, yielding commences at the outer surface where the stresses satisfy the inequality $\sigma_\theta = \sigma_z > \sigma_r = 0$. This stress state leads to the elastic limit heat load for both von Mises' and Tresca's criteria

$$Q_1 = \frac{2(1-a^2)(1-\nu)}{1/4 - a^2 + 3/4a^4 - a^4 \ln a}. \tag{66}$$

Taking the Poisson's ratio as $\nu = 0.3$, the elastic limit heat loads for cylinders and tubes of different inner radii are calculated and the results are presented in Table 1.

Table 1. Elastic limit heat loads.

	Fixed End		Free End
a	von Mises	Tresca	Both criteria
0	4.6667	4.6667	5.6
0.1	4.0352	3.5074	5.7677
0.2	4.6258	4.0136	6.2870
0.3	5.5963	4.8497	7.2458
0.4	7.1519	6.1943	8.8650
0.5	9.7595	8.4523	11.641

A run is performed to compute the stresses and displacement in a cylinder with free ends at the elastic limit load $Q_1 = 5.6$. Iterations start with $\epsilon_0^0 = 0.5$ and converge to $\epsilon_0 = 0.70000$ within 3 iterations. The analytical result is $\epsilon_0 = 0.7$. The corresponding stresses and displacement are plotted in Figure 1(a). In this figure, solid lines represent numerical results and dots analytical results. Perfect agreement with the analytical solution is obtained. The stress variable ϕ in this figure is computed from

$$\phi = \sqrt{\frac{1}{2}\left[(\sigma_r - \sigma_\theta)^2 + (\sigma_r - \sigma_z)^2 + (\sigma_\theta - \sigma_z)^2\right]}, \tag{67}$$

which is simply the yield stress σ_y in the plastic zone. Note that $\phi = 1$ at the elastic-plastic border and $\phi < 1$ in the elastic region. As seen in Figure 1(a), for a cylinder with free ends $\phi = 1$ at the surface ($r = 1$) and hence plastic deformation commences at this location for loads $Q > Q_1$ and the plastic region formed here propagates toward the center with increasing thermal loads.

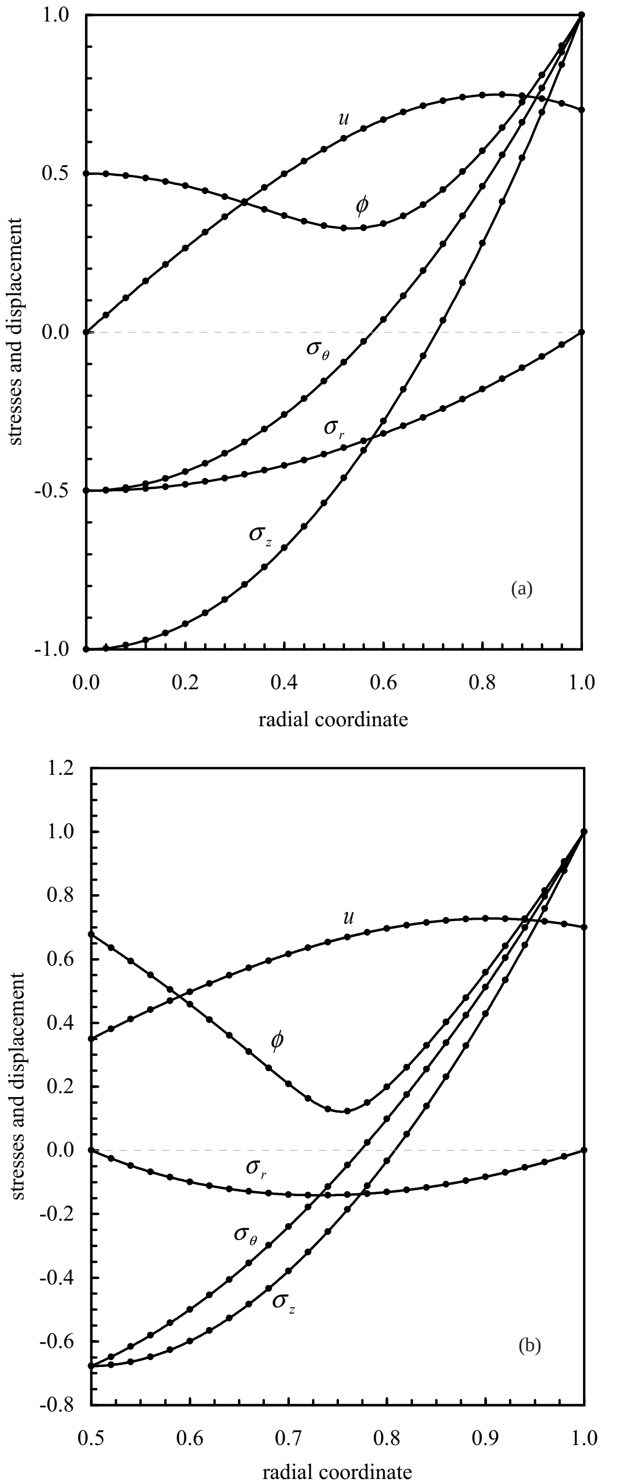

Figure 1. Stresses and displacement in (a) a cylinder with free ends at elastic limit heat load $Q = 5.6$, (b) a tube with free ends at elastic limit heat load $Q = 11.641$.

For a tube of inner radius $a = 0.5$ with free ends, the elastic limit heat load, as given in Table 1, is $Q_1 = 11.641$. The stresses and displacement at this load are calculated and plotted in Figure 1(b). Again, numerical and analytical solutions agree perfectly. Furthermore, it is evident from this figure that $\phi = 1$ at the outer surface pointing the location of formation of plastic deformation. These sample calculations reveal that the numerical solution algorithm performs very well and that the computer code that implements this algorithm is functioning properly.

Results and Discussion

Before the results of nonlinear hardening structures are presented, comparisons will be made with published analytical solutions based on Tresca's yield criterion. The stresses in a uniform heat generating, elastic ideally plastic cylinder with free ends were calculated by Orcan (1994a). Since the present model is not specifically designed for ideally plastic materials, it is impossible to take $H = 0$ exactly for computational reasons. However, material behavior of this type may be simulated by assigning $m = 1$ and using sufficiently small H. Using the parameters of Orcan (1994a), $Q = 16.2$, $\nu = 0.295$ and also $m = 1$ and $H = 10^{-5}$, the corresponding stresses, displacement and plastic strains are computed. Figures 2(a) and (b) show the results of this computation (solid lines) in comparison to those of Orcan (1994a) (dots). The stresses and displacement, as shown in Figure 2(a), compare well. Conversely, as seen in Figure 2(b), the comparison concerning the plastic strains is poor. The fact that the cylinder is composed of 3 regions, an inner plastic, an elastic and an outer plastic is evident from Figure 2(a), through a look at the variation of ϕ. In addition $\phi = 1$ in both plastic regions is the result of nonhardening behavior of material.

Another analytical solution for an ideally plastic material was derived by Orcan and Gülgeç (2001) for a tube with free ends using the temperature distribution given by Eq. (56). The results of the calculations are compared with their solution for the stresses and displacement in Figure 3(a) and plastic strains in Figure 3(b). Again, dots represent the analytical solution. The parameters used are $a = 0.2$, $Q = 20.0$, $\nu = 0.295$, $H = 10^{-5}$. In contrast to the free end cylinder solution, the agreement between 2 solutions as to plastic strains is satisfactory.

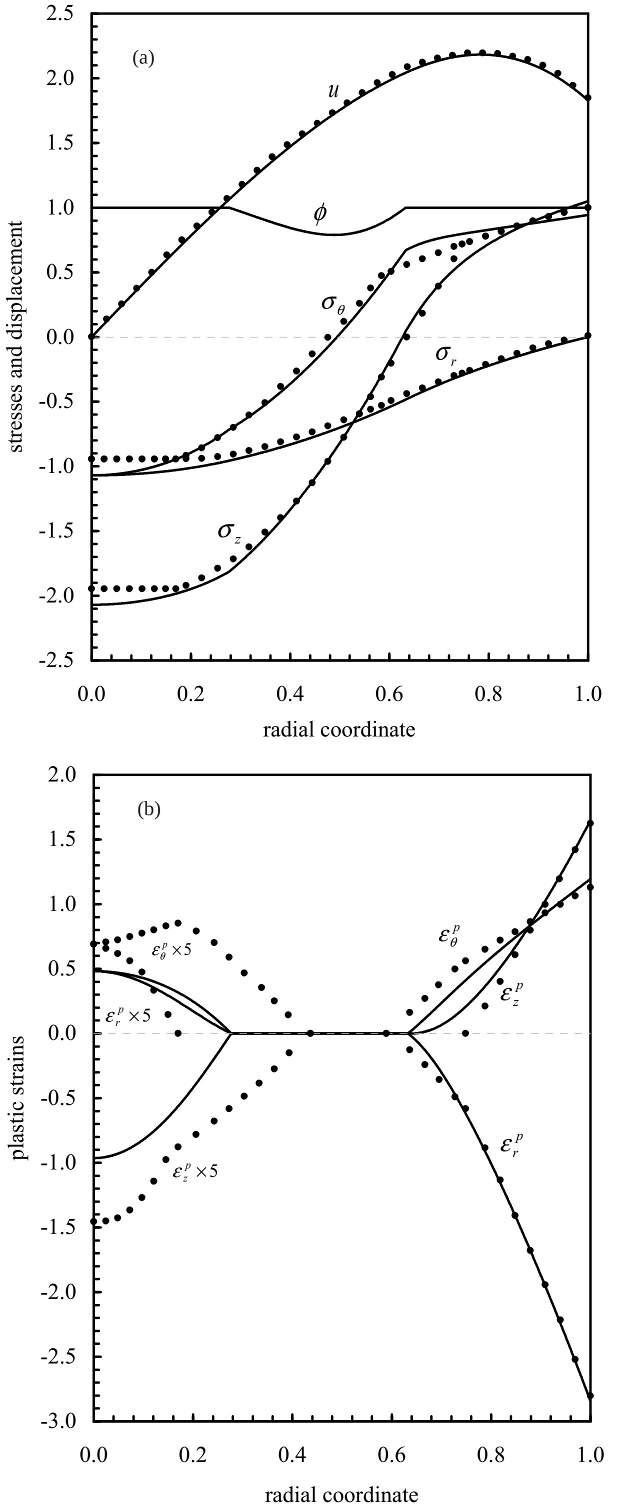

Figure 2. (a) Stresses and displacement, (b) plastic strains in elastic ideally plastic cylinder with free ends at $Q = 16.2$. Dots represent the analytical solution of Orcan (1994a).

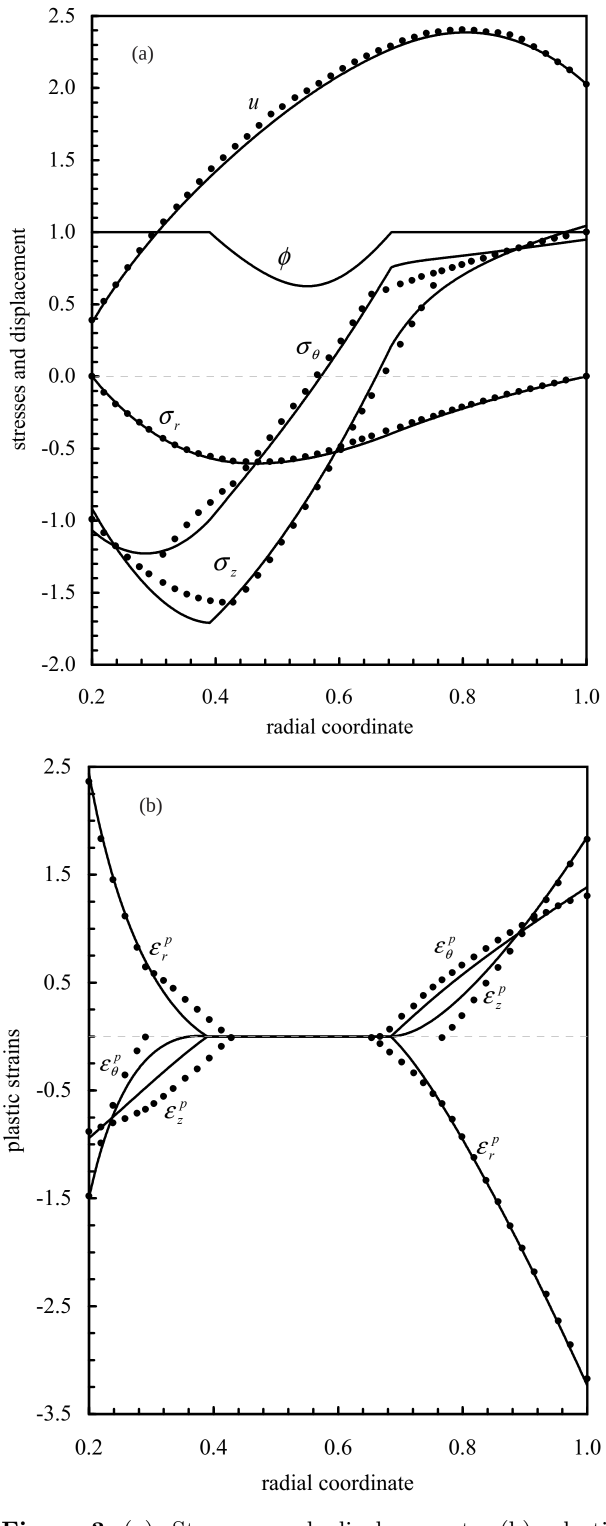

Figure 3. (a) Stresses and displacement, (b) plastic strains in elastic ideally plastic tube with free ends at $Q = 20$. Dots represent the analytical solution of Orcan and Gülgeç (2001).

The thermoplastic response of a linear strain hardening cylinder with fixed ends was studied by Sener and Eraslan (2003). All stages of elastic-plastic deformation were treated analytically, from purely elastic to fully plastic, by Sener and Eraslan (2003), employing the temperature field (49). Taking $Q = 5.6054$, $\nu = 0.295$, $m = 1$ and $H = 0.25$ the stresses and displacement are calculated and compared with the analytical result from Sener and Eraslan (2003) in Figure 4(a). Moreover, the propagation of the elastic-plastic border with the increasing values of heat load is also calculated and the result is plotted in Figure 4(b). The dots belong to the analytical result of Sener and Eraslan (2003). As seen in this figure, plastic deformation commences at the center of the cylinder at $Q = 4.6667$ (see Table 1) and propagates toward the surface as the heat load is increased. When the heat load reaches another critical value, Q_s, a second plastic region develops at the surface. The present model predicts $Q_s = 6.2795$, while the analytical finding is 5.6103. Moreover, the cylinder becomes just fully plastic at $Q_{fp} = 6.9773$, though $Q_{fp} = 6.8412$ is reported in Sener and Eraslan (2003), based on the analytical solution. Figure 4(b) also shows that the elastic-plastic border advances more rapidly by Tresca's criterion than by that of von Mises', and hence more conservative limit heat loads are predicted.

The work of Orcan (1994a) was recently extended to linear hardening by Sener (2003). A final comparison is made with the results of Sener (2003). These comparisons are shown in Figures 5(a) and (b). Model predictions for the stresses and displacement corresponding to the parameters $Q = 10$, $\nu = 0.295$, $m = 1$ and $H = 0.25$ are compared to those of Sener (2003) in Figure 5(a), and for the plastic strains in 5(b). This comparison and the ones discussed above verify the present elastoplastic model on a different class of problems and for a wide range of values of parameters.

To give an example regarding nonlinearly hardening thermal stress calculation, we consider a uniform heat generating cylinder with fixed ends. The deformation behavior of this cylinder has been explained above with reference to the analytical work of Orcaw (1994) and temperature distribution (49). The cylinder with fixed ends becomes partially plastic for the loads $Q > 4.6667$. Taking $\nu = 0.3$, $H = 0.4$ and $m = 0.5$, and assigning $Q = 6.85$, the elastic-plastic stresses and displacement in a nonlinearly hardening cylinder are computed and plotted

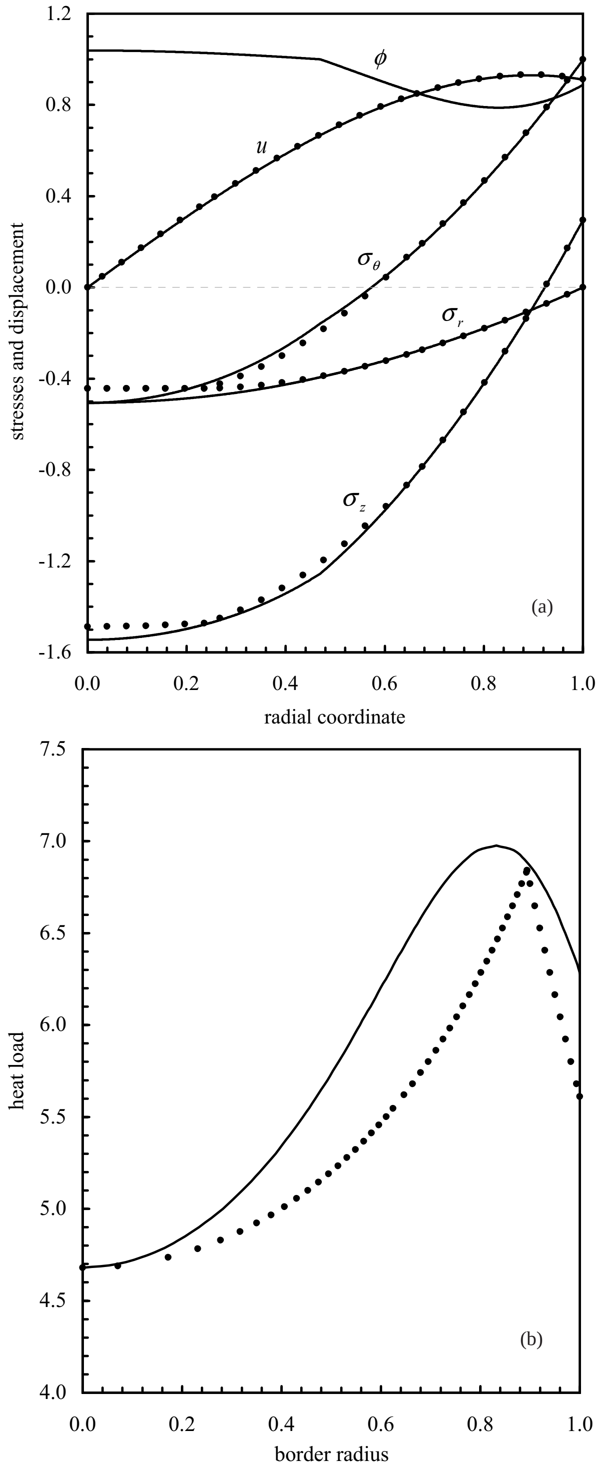

Figure 4. (a) Stresses and displacement at $Q = 5.6054$, (b) propagation of elastic-plastic border radius in a linearly hardening cylinder with fixed ends. Dots represent the analytical solution of Sener and Eraslan (2003).

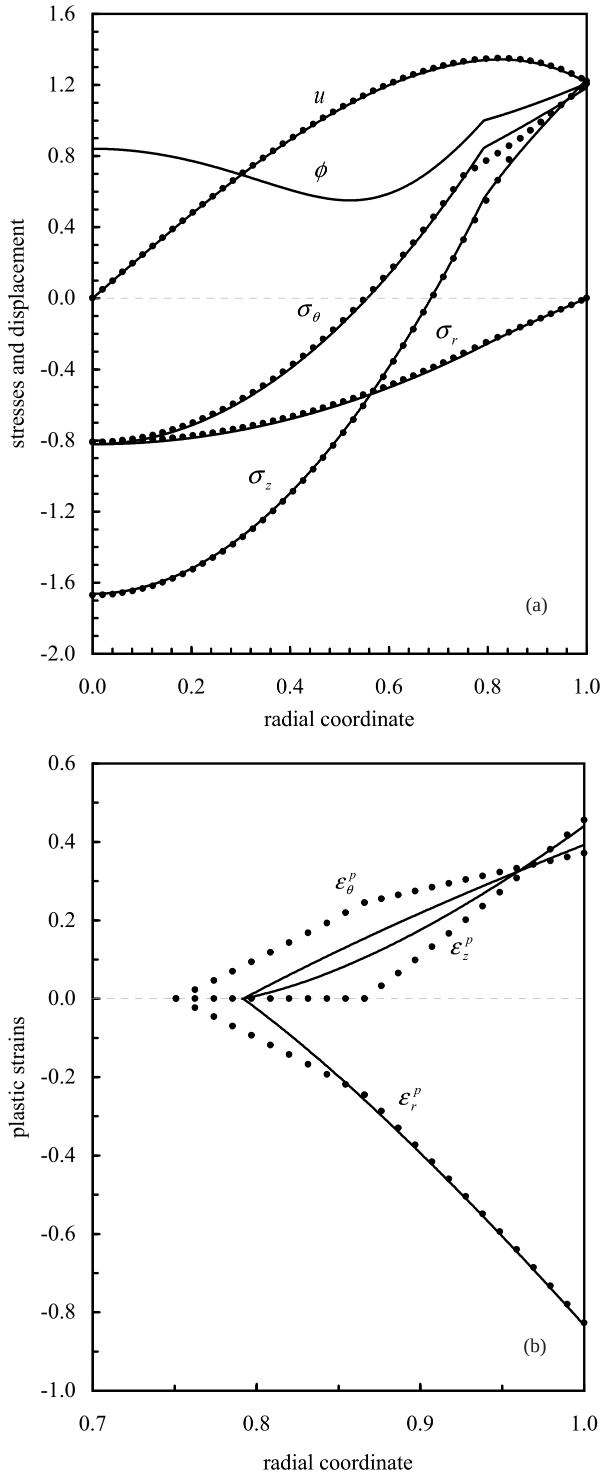

Figure 5. (a) Stresses and displacement, (b) plastic strains in a linearly hardening cylinder with free ends at $Q = 10$. Dots represent the analytical solution of Sener (2003).

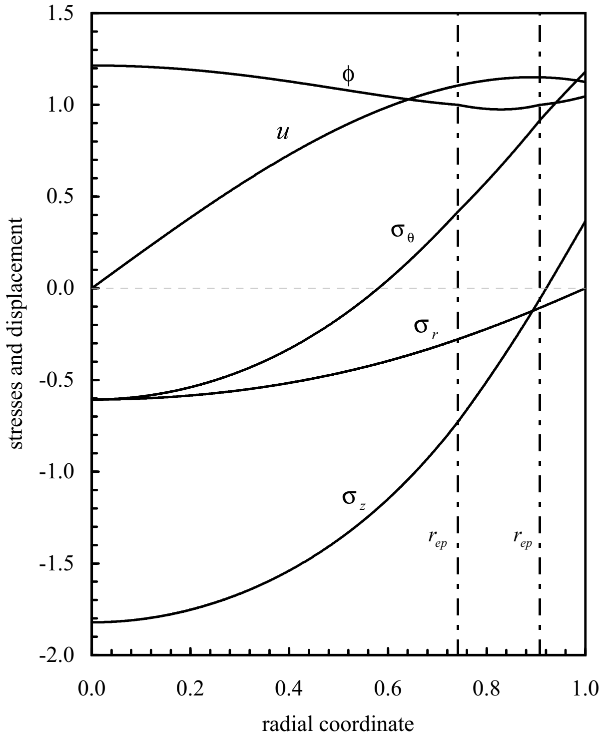

Figure 6. Stresses and displacement in a nonlinearly hardening cylinder with fixed ends at $Q = 6.85$.

in Figure 6. Under this load, the cylinder is composed of 3 different regions: an inner plastic region in $0 \leq r \leq 0.74169$, an elastic region in $0.74169 \leq r \leq 0.90811$ and an outer plastic region in $0.90811 \leq r \leq 1$. An elastic-plastic border in Figure 6 is designated by the symbol r_{ep}. Additional runs are performed for this system to investigate the effect of material parameters H and m on plastic strains. The results of these calculations are depicted in Figures 7 and 8. In both, $\nu = 0.3$ and $Q = 6.85$. Figure 7 exemplifies the effect of the hardening parameter H on plastic strains corresponding to $m = 0.5$, while Figure 8 demonstrates the effect of m corresponding to $H = 0.4$. As seen in these figures, both parameters affect plastic strains significantly and there are correspondingly larger plastic strains for smaller values of H and larger values of m. It is also seen that the widths of inner and outer plastic zones are both notably affected by the change in either H or m. The propagation of an elastic plastic border with increasing values of heat load is shown in Figure 9. In Figure 9(a), H is kept constant at 0.4 and m is used as a parameter. As seen in this figure, the fully plastic limit heat load Q_{fp} increases in the direction of decreasing m. The hardening parameter H is used as a parameter for $m = 0.5$ in Figure 9(b). As seen in Figure 9, the effect of parameters H and m on the propagation of elastic-plastic interface becomes significant as the fully plastic limit is approached.

The fully plastic limit of the cylinder with fixed ends corresponding to the values of parameters $\nu = 0.3$, $H = 0.4$, $m = 0.5$ is calculated as $Q_{fp} = 7.0099$. The stresses and displacement at this limit heat load are presented in Figure 10. The elastic region shrinks to a surface at $r = r_{ep}$ where both plastic regions join each other. A parametric analysis is carried out to investigate the effect of material parameters H and m on the plastic limit heat load Q_s as well as on the fully plastic limit heat load Q_{fp}. Note again that, Q_s is the critical load at which plastic deformation sets in at the free surface. Figure 11 shows the result of this analysis. Variation of Q_s with m using H as a parameter is plotted in Figure 11(a) whereas variation of Q_{fp} is plotted in Figure 11(b). As seen in these figures, although both Q_s and Q_{fp} increase with increasing H and decreasing m, these effects are more pronounced on the fully plastic limit Q_{fp}.

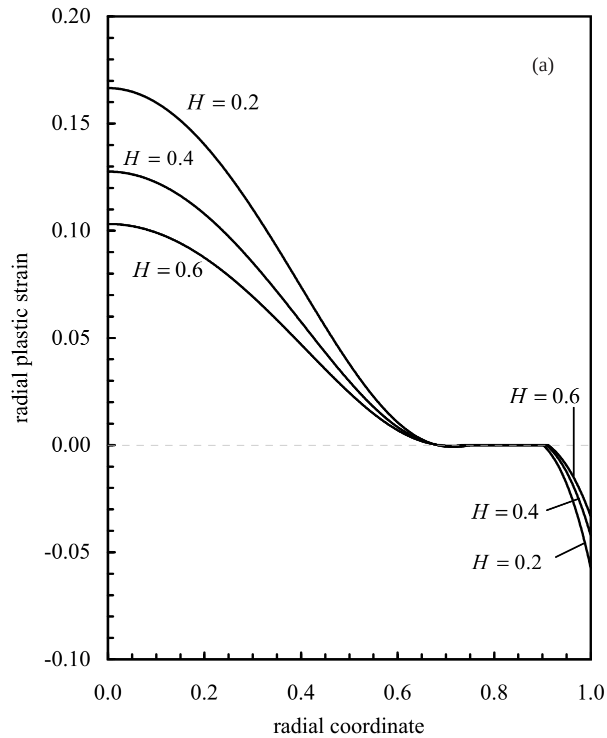

Figure 7. (a) Radial, (b) circumferential and (c) axial plastic strains in a nonlinearly hardening cylinder with fixed ends for different values of H and $m = 0.5$ at $Q = 6.85$.

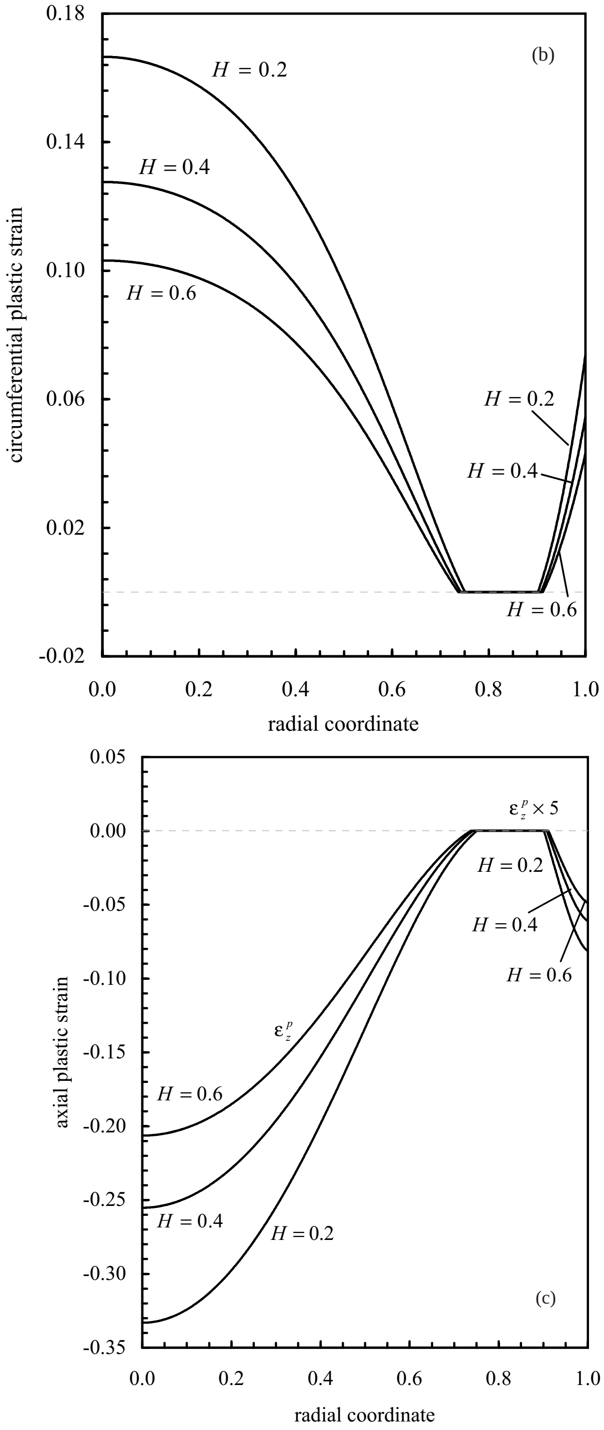

Figure 7. Contunied.

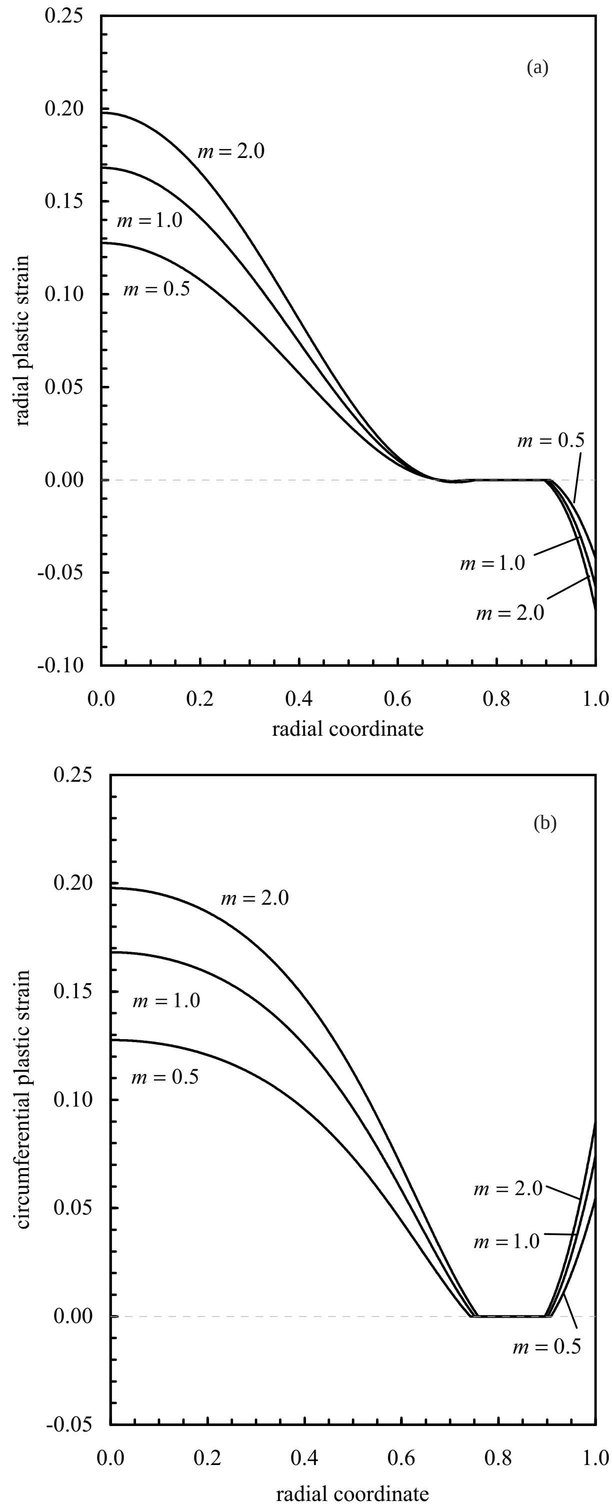

Figure 8. (a) Radial, (b) circumferential and (c) axial plastic strains in a nonlinearly hardening cylinder with fixed ends for different values of m and $H = 0.4$ at $Q = 6.85$.

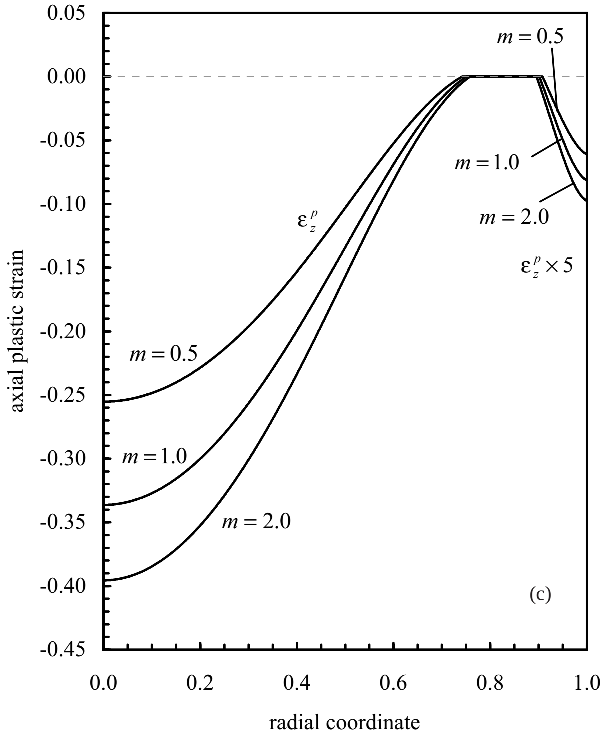

Figure 8. Contunied.

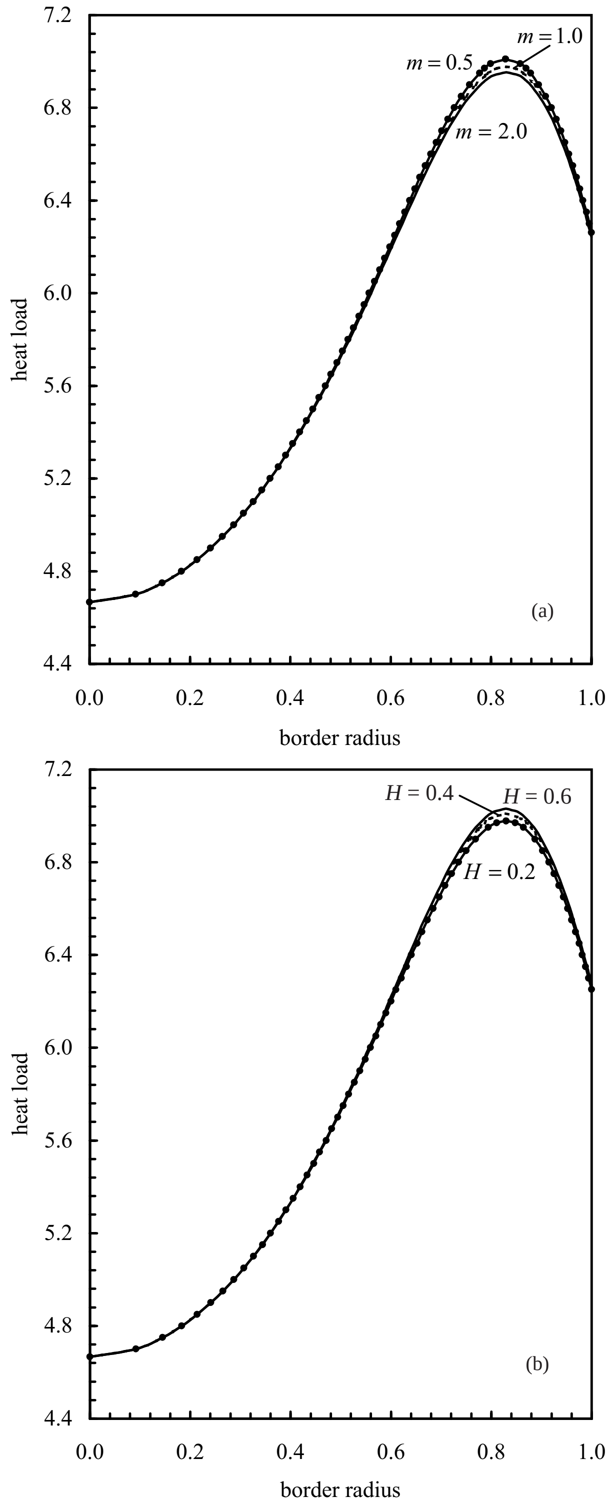

Figure 9. Propagation of elastic-plastic border radius for (a) different values of m and $H = 0.4$, (b) for different values of H and $m = 0.5$ in a nonlinearly hardening cylinder with fixed ends.

In engineering applications, the system is subjected to repeated stress cycles by loading and unloading. The residual stresses occurring during the unloading process and the possibility of alternating the plastic response of the system is also investigated. To this end, the residual stresses due to complete unloading of the thermal load $Q = 6.85$ (Figure 6) are calculated by subtracting the stresses and displacement corresponding to unrestricted elastic behavior from elastic-plastic ones at the same load parameter. Of course, this calculation procedure holds true only when the residual stresses do not exceed the yield limit (Orcan, 1994b). Residual stresses and displacement are plotted in Figure 12(a). In this figure, the nondimensional stress components are designated by σ_j^0 and displacement by u^0 to imply stand-still. The stress variable ϕ^R is calculated from Eq. (67) with σ_j replaced by σ_j^0. Since $\phi^R < 1$, unloading occurs elastically and reversed plastic flow (secondary plastic flow) does not take place. The residual plastic strains are not altered and are as given in Figure 7. The axial stress is again maximum at the axis, but this time it is tensile. Upon reloading, superposition of the stresses due to the applied thermal load on the

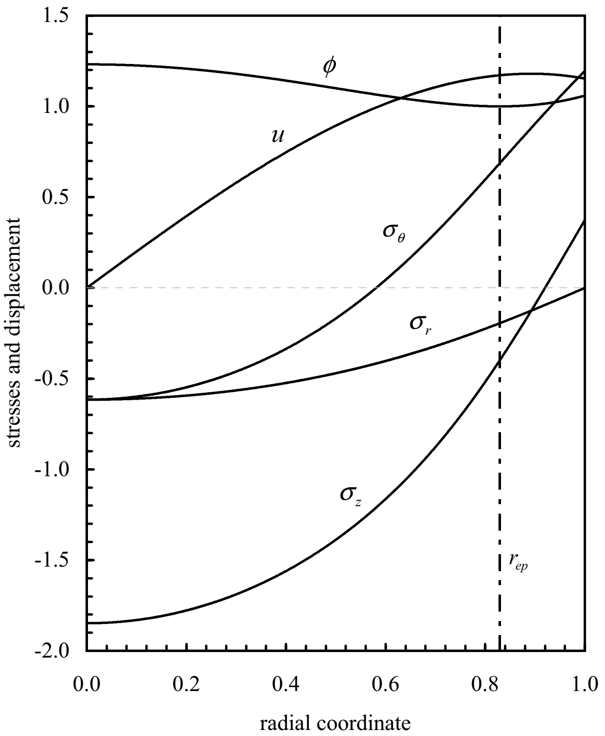

Figure 10. Stresses and displacement at fully plastic limit $Q_{fp} = 7.0099$ in a nonlinearly hardening cylinder with fixed ends.

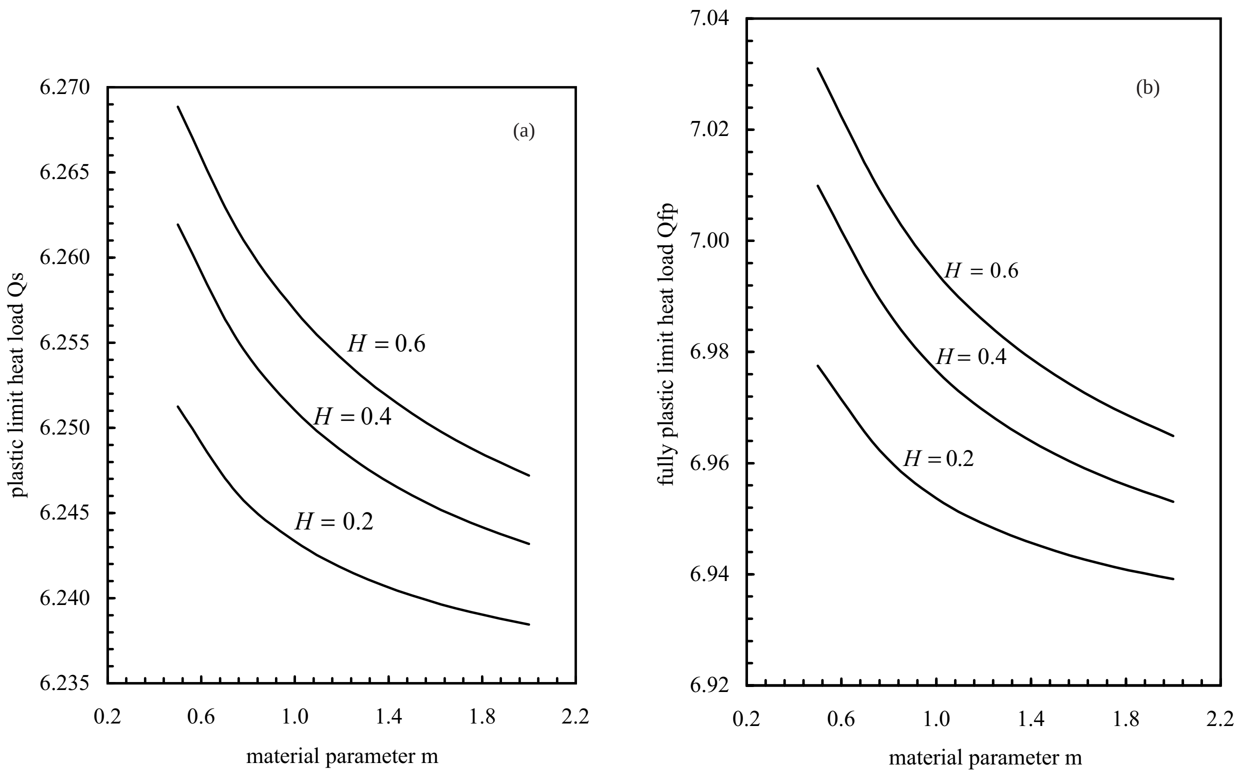

Figure 11. Dependence of the plastic flow limits (a) Q_s, (b) Q_{fp} on material parameters H and m for a cylinder with fixed ends.

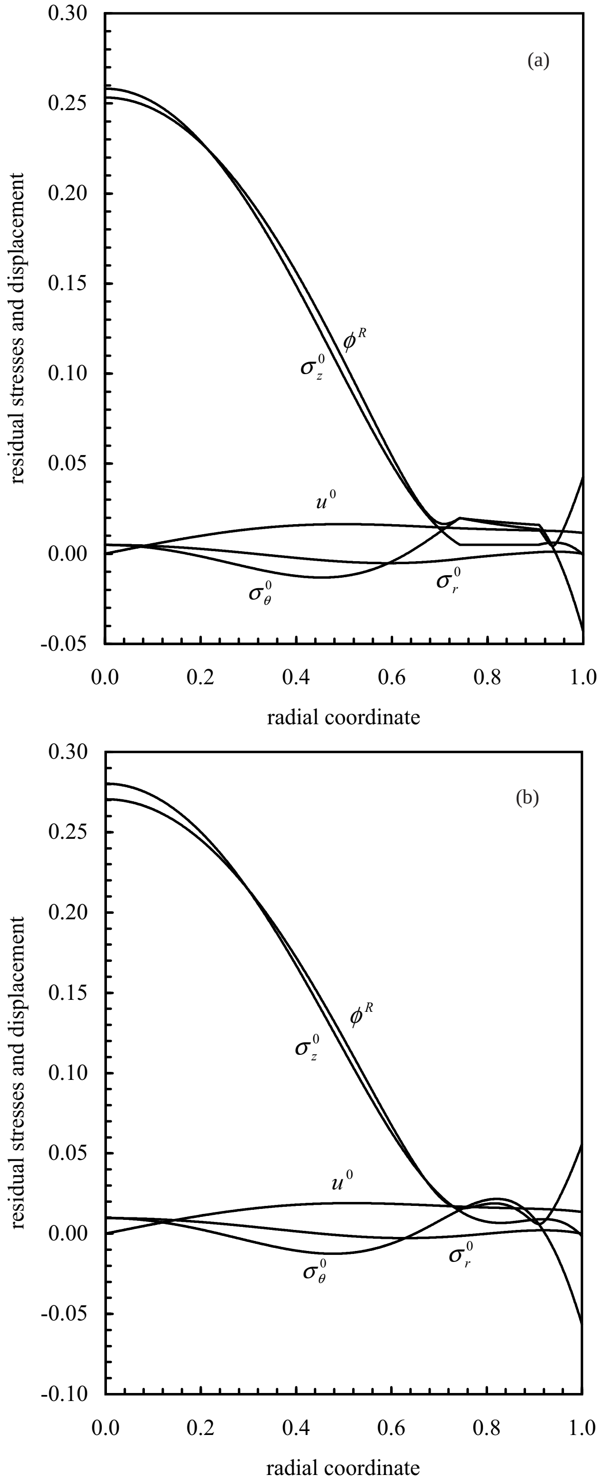

Figure 12. Residual stresses and displacement upon removal of (a) elastic-plastic heat load $Q = 6.85$, (b) fully plastic limit heat load $Q_{fp} = 7.0099$ in a nonlinearly hardening cylinder with fixed ends.

state of residual stress does not lead to an extension of the yield surface. The residual stresses and residual displacement on unloading of the fully plastic load $Q_{fp} = 7.0099$ are shown in Figure 12(b). As seen in this figure, ϕ^R is still less than 1 and hence secondary plastic flow does not occur. Residual stresses are not excessive and shakedown to elastic response takes place upon unloading and reloading.

Concluding Remarks

Taking nonlinear hardening into account, an easy-to-handle unified computational model is developed to solve a class of plane strain thermal stress problems of engineering interest. The model is based on von Mises' yield criterion, the deformation theory of plasticity, and a Swift-type hardening law. A nonlinear shooting method using Newton iterations with numerically generated tangents is developed and used throughout this work for the simultaneous solution of governing equations. The computational model is verified in comparison to analytical results in the elastic and elastic-plastic states.

This paper represents an extension of the previous studies in theoretical analysis of elastic-plastic plane strain thermal stress problems to include von Mises' yield criterion and nonlinear isotropic strain hardening. Von Mises' yield criterion is known to comply better with experimental observations, but its use is essentially numerical because of its nonlinear form. This numerical treatment allows the incorporation of nonlinear hardening laws to handle more realistic elasto-plastic deformations. In this paper, Swift's hardening law is used. However, the model is designed in such a way that any other hardening law or polynomial strain-yield stress relations can easily be incorporated. The results presented in this work were obtained by a comparatively easy procedure based on a single nonlinear ordinary differential equation, and thus they may also serve as a countercheck for purely numerical studies by the finite element method.

Finally, it should be pointed out that the consideration of temperature dependent material properties in thermal stress calculations results in more dependable predictions (Orcan and Eraslan, 2001). The success of the present model promises the incorporation of temperature dependent material properties in the near future.

References

Boley, B.A. and Weiner, J.Fr., Theory of Thermal Stresses, Wiley, New York, 1960.

Eraslan, A.N., "Thermally Induced Deformations of Elastic-Plastic Composite Tubes Subjected to a Nonuniform Heat Source". Journal of Thermal Stresses 26, 167-193, 2003.

Eraslan, A.N. and Orcan, Y., "Thermoplastic Response of a Linearly Hardening Cylinder Subjected to Nonuniform Heat Source and Convective Boundary Condition". Mechanics Based Design of Structures and Machines 32, 133-164, 2004.

Eraslan, A.N., Sener, E. and Argeso H., "Stress Distributions in Energy Generating Two-Layer Tubes Subjected to Free and Radially Constrained Boundary Conditions". International Journal of Mechanical Sciences 45, 469-496, 2003.

Gülgeç, M. and Orcan, Y., "On the Elastic-Plastic Deformation of a Centrally Heated Cylinder Exhibiting Linear Hardening". Journal of Applied Mathematics and Mechanics (ZAMM) 79, 493-498, 1999.

Hindmarsh, A.C., ODEPACK: A Systematized Collection of ODE Solvers. In: Scientific Computing, (Stepleman, R.S., ed.) North Holland, Amsterdam, 1983.

Orcan, Y. and Gamer, U., "Elastic-Plastic Deformation of a Centrally Heated Cylinder". Acta Mechanica 90, 61-80, 1991.

Orcan, Y., "Thermal Stresses in a Heat Generating Elastic-Plastic Cylinder with Free Ends". International Journal of Engineering Science 32, 883-898, 1994a.

Orcan, Y., "Residual Stresses and Secondary Plastic Flow in a Heat Generating Elastic-Plastic Cylinder with Free Ends". International Journal of Engineering Science 33, 1689-1698, 1994b.

Orcan, Y. and Eraslan, A.N., "Thermal Stresses in Elastic-Plastic Tubes with Temperature-Dependent Mechanical and Thermal Properties". Journal of Thermal Stresses 24, 1097-1113, 2001.

Orcan, Y. and Gülgeç, M., "Elastic-Plastic Deformation of a Tube with Free Ends Subjected to Internal Heat Generation". Turkish Journal of Engineering and Environmental Sciences 25, 1-10, 2001.

Sener, E., Thermal Stresses in a Heat Generating Linearly Hardening Cylinder with Free Ends, MSc Thesis. Department of Engineering Sciences, Middle East Technical University, Ankara, Turkey, 2003.

Sener, E. and Eraslan, A.N., (in Turkish) "Lineer Olarak Pekleşebilen Uçları Sabit Bir Silindirin Termo-Elasto-Plastik Analitik Çözümü". Proceedings of the 13th National Congress on Mechanics, Gaziantep, Turkey, 727-736, 2003.

Uğural, A.C. and Fenster, S.K., Advanced Strength and Applied Elasticity, 3rd ed., Prentice-Hall, London, 1995.

Timoshenko, S. and Goodier, J.N., Theory of Elasticity, 3rd ed., McGraw-Hill, New York, 1970.